Disinfection '98

The Latest Trends in Wastewater Disinfection: Chlorination vs. UV Disinfection

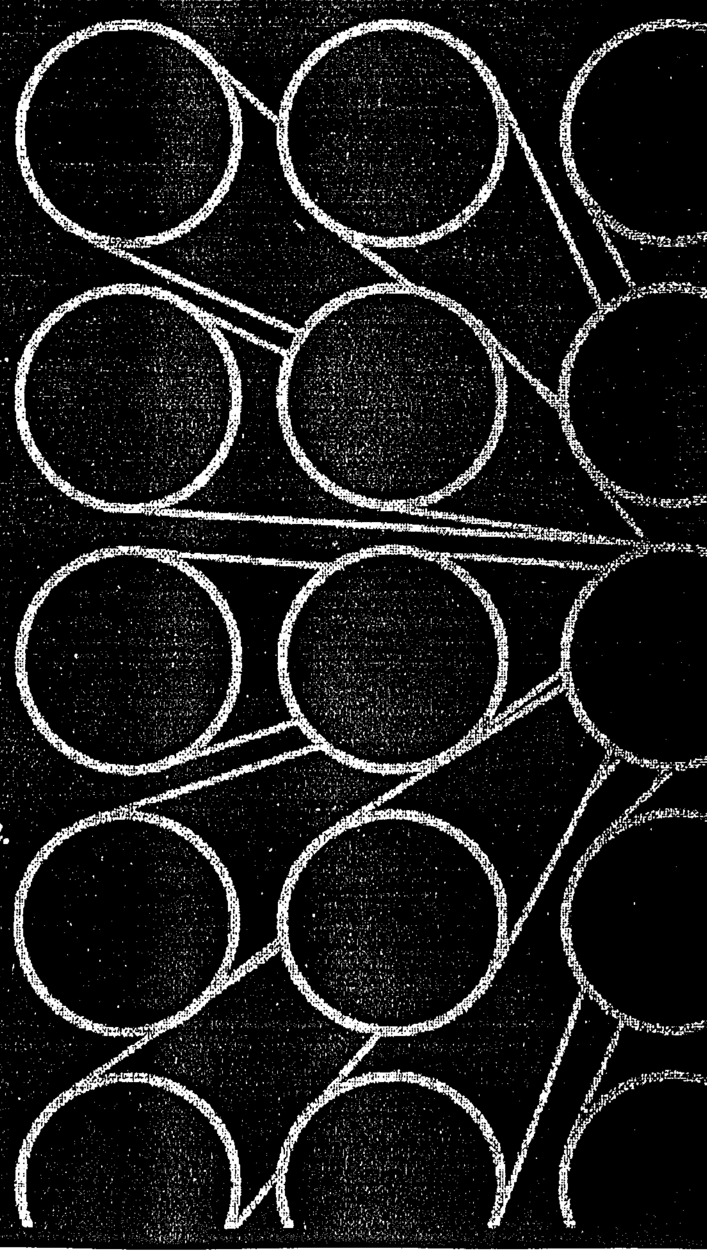

April 19 - 22, 1998
Omni Inner Harbor
Baltimore, Maryland U.S.A.

Held in cooperation with the Chesapeake Water Environment Association.

Water Environment Federation®
Preserving & Enhancing the Global Water Environment

CHALLENGES IN GUARANTEEING THE VIRUS DISINFECTION PERFORMANCE OF MICROFILTRATION/ULTRAVIOLET IRRADIATION SYSTEMS IN WASTEWATER RECLAMATION

R. Iranpour, A. Magallanes, T. Jugo,K. Ludwig, C. Mansell Jr., K. Flaig
Wastewater Res. Grp./ WESD/ Sanitation/ City of Los Angeles

ABSTRACT

A study of virus removal effectiveness of microfiltration (MF) was carried out at the Terminal Island Treatment Plant of Los Angeles. Comparing the results with several similar studies by others shows variability over several log units (orders of magnitude). This is significant because some programs for reclamation are now considering microfiltration followed by ultraviolet (UV) irradiation as the final two steps in treatment, and small concentrations of active pathogenic viruses are enough to compromise the safety of reclaimed wastewater for many purposes. Hence, the ability of a tertiary treatment system to remove or inactivate almost all of the viruses remaining after previous treatment is a key aspect of overall reclamation system performance. The variability of microfiltration of viruses makes overall system performance dependent on the inactivation effectiveness of the subsequent UV irradiation step. A recent study made in San Francisco provides encouraging evidence that a large degree of inactivation can be achieved in this highly filtered water with much lower doses than those currently mandated by regulations based on research on disinfecting secondary effluent. However, the relationship between dose and inactivation appears to depart from first order kinetics. The dose estimates are based on assuming plug flow, and since hydrodynamic studies show evidence of departures from plug flow in UV reactors, the apparently anomalous kinetics are tentatively explained by hydrodynamic effects. These are subject to improvement by modification of UV reactor design. Design of MF/UV systems that successfully meet disinfection standards depends on adequately understanding the phenomena within these units that add complexity to their behavior.

KEYWORDS

hydrodynamics, plug flow, boundary layer, UV reactor, reclamation, microfiltration

INTRODUCTION

Increased quantities of wastewater will be reclaimed in the future, as populations continue to increase, and natural water supplies in many places remain fixed. For many purposes, reducing the concentration of active pathogenic viruses to a very low level is necessary, so that the reclamation system must perform some combination of removal and inactivation. Several programs for increasing reclamation are currently considering performing disinfection by ultraviolet irradiation instead of chemical disinfection because the higher cost of a UV system is considered less important than its safety advantages over the use of chemicals and because it does not contaminate the water with chlorinated disinfection by-products.

Most of these UV systems are low-pressure, low-intensity systems that are subject to fouling, but preceding such a system with a microfiltration unit greatly reduces the fouling by removing both the vast majority of the bacteria and many particles that could nourish them. Hence, many planned reclamation systems have MF/UV combinations, as the final operations on the water.

Evidently, since viruses with diameters of some tens of nanometers are much smaller than the nominal pore size of several hundred nanometers in microfiltration membranes, free floating viruses might be expected to pass through with little difficulty. However, viruses attached to larger particles would be stopped, and this might also happen if the membrane and the viruses interact in any way other than simple mechanical removal. This possibility cannot be ruled out *a priori*, since locally charged areas on the virus surfaces and the membrane molecules might attract each other, and viruses might also stick to deposits of bacterial material on the membrane.

Hence, the effectiveness of microfiltration in virus removal has been studied by several groups of investigators (Jolis and Hirano, 1993; Willinghan et al., 1992; Water Board, 1992), including a recent study at the Terminal Island Treatment Plant by the Research Group of the Los Angeles Sanitation (1997). Some of these studies have used naturally occurring viruses and some have used seeded viruses, so the comparison of their results is not biased by either experimental technique. As described below in the "Virus Microfiltration Studies" section, these studies collectively show that microfiltration may reduce the virus concentration by anywhere from less than 1 log unit (or order of magnitude) to 4 log units, and that the amount removed varies with time for individual units.

These results enhance the significance of Jolis and Hirano (1993), which is a study of the disinfection effectiveness of a combined MF/UV system, carried out at the Southeast Plant (SEP) of the City and County of San Francisco. Although present California regulations (Wastewater Reclamation Criteria , 1978), Title 22 of the California Code of Regulations, recommended a UV dose of at least 140 mW-S/cm^2 to achieve specified inactivation of coliform bacteria and colliphage viruses, Jolis and Hirano observed adequate virus reduction at an estimated dose of 88 mW-s/cm^2. Since microfiltration removes most of the particles that could scatter incoming light, or provide shelter to viruses, and since the 140 mW-s/cm^2 standard is based on experiments with secondary effluent that had not been microfiltered, the greater effectiveness of UV irradiation of microfiltered water is consistent with expectations.

A much more surprising result of this report is the apparent independence of disinfection from dose, and its apparent dependence only on the number of lamp banks through which the water passes. This violates the first-order kinetics theory of disinfection, which has previously been widely accepted as the fundamental process in UV reactors, based on a combination of both plausible theoretical arguments and abundant previous experimentation.

The most plausible present interpretation of these results is that first-order kinetics remains valid at the microscopic level, and that the apparent dose-independence observed by Jolis and Hirano is the result of hydrodynamic effects in the UV reactor that invalidate the simple formula, based on the assumption of perfect plug flow, by which they estimated the doses. They had lamps with fixed intensities, as is true for all UV disinfection systems known to the authors, and so Jolis and Hirano sought higher doses by reducing the average velocity through their UV reactor. However, other studies show that at velocities comparable to those they used, boundary layer effects reduce the cross-sectional area through which most of the water flows among the lamps, so that the assumption of plug flow no longer holds within a lamp bank of present design.

Two conclusions follow:

a. that modified UV reactor design could provide a closer approximation to plug flow, and hence more reliable estimates of dosage;
b. that the actual dose applied to most of the water is less than the estimate from the plug flow assumption, offering the potential for greater energy savings than implied by assuming plug flow.

Hence, it appears that the efficiency of MF/UV systems that meet Title 22 or comparable standards may improve significantly with improved understanding of the phenomena within each type of unit, and perhaps with modification of current designs to enhance plug flow in UV reactors or to enhance virus removal in microfiltration.

VIRUS MICROFILTRATION STUDIES

Figures 1a and 1b are from Iranpour et al. (1997), showing the results of two days of the tests made at TITP on a Memcor microfiltration unit. These tests were made with seeded viruses at a relatively high concentration, as shown in Table 1. As Figure 1a shows, the removal factor changed substantially in a few hours on March 27, but it was always significantly larger than on April 3, as shown in Figure 1b.

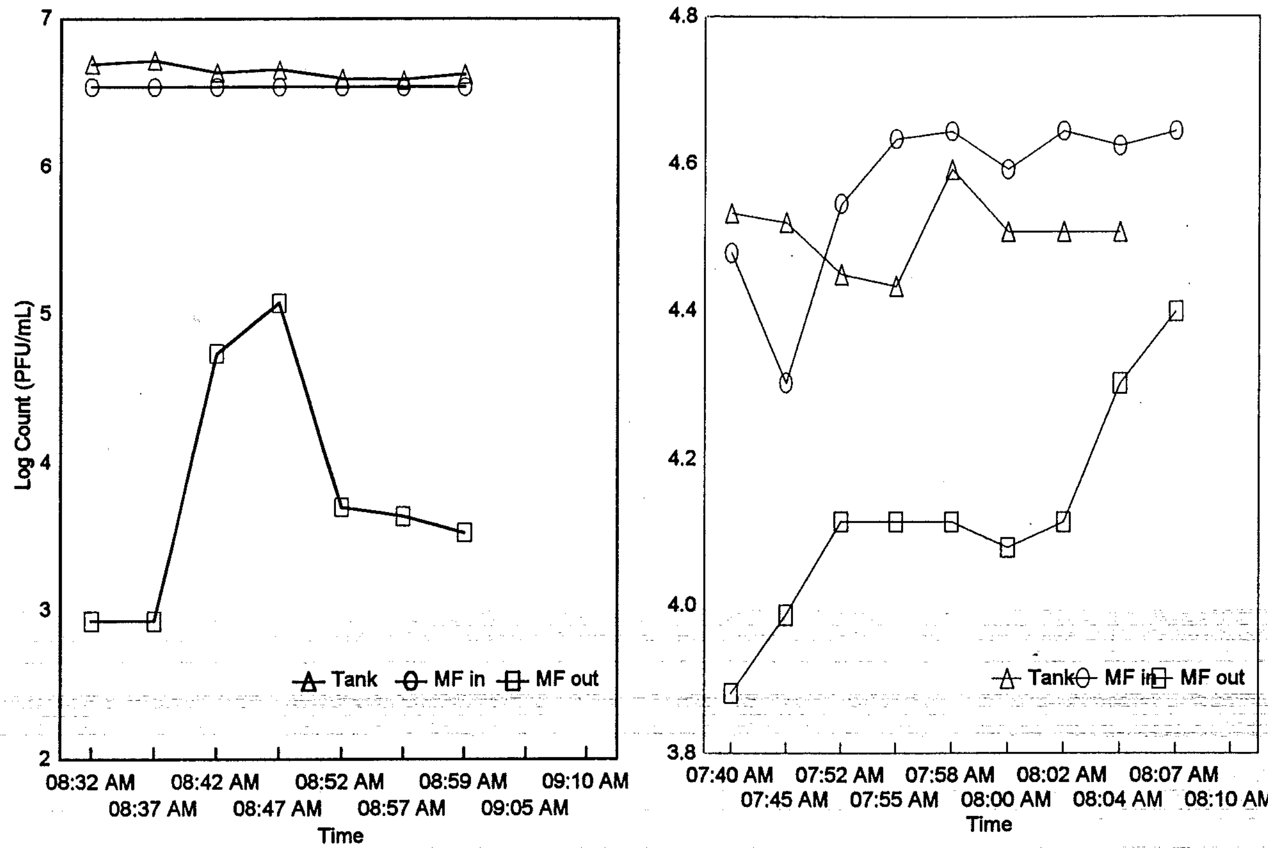

(a) March 27, 1996

(b) April 3, 1996

Figure 1—Removal of MS2 phages for Memcor microfiltration, Terminal Island Plant, Los Angeles.

These results are apparently typical for seeded virus experiments, as indicated by Figure 2, which condenses three days of seeded virus experiments done by Jolis and Hirano. Their description of the operation of their microfiltration unit, including the backwashing process with compressed air, indicates that it is either a Memcor unit or extremely similar. Their results also show variability over several log units both within a day and between days.

Figure 3 adapted from Willinghan et al. (1992) shows results obtained for naturally present viruses with a Memcor unit at Baltimore, over a period of 400 days of operation. The weekly measurements show substantial variation in the natural viruses population in the feed, but much larger variation in the filtrate, and hence variation in filtration effectiveness of several log units, as was seen in the seeded experiments.

These data are obtained by sampling the filtrate and applying it to culture plates with layers of coliform bacteria growing on them to determine the number of plaques formed by the action of coliphage viruses in the filtrate (Adams, 1959). The same kind of assay is used for tests of natural viruses in the feed, and in tests to verify the concentration guaranteed by the supplier of the seed viruses in the seeded tests. Thus, what is actually counted is not individual viruses but plaque forming units per hundred mL, without knowing how many viruses form the unit. Since the viruses are reproduced by multiplication in coliform bacteria at least some of the units consist of bits of bacterial membrane with many viruses attached.

Table 1—Summary of virus concentrations for experiments in Figure 1, Terminal Island Plant, Los Angeles.

	BioVir Laboratory		Environmental Monitoring Division Laboratory	
	Virus		Sample mean ± standard deviation	
Date	Concentrate	Nominal	Tank	MF inlet
03/27/96	20	5.0E+11	(4.55±0.46)E+06	(3.50±0.00)E+06[(a)]
04/03/96	2	5.0E+10	(3.2±0.34)E+04	(3.79±0.78)E+04

(a) On 03/27/96 EMD laboratory staff missed the correct dilution. They provided only one approximate count.

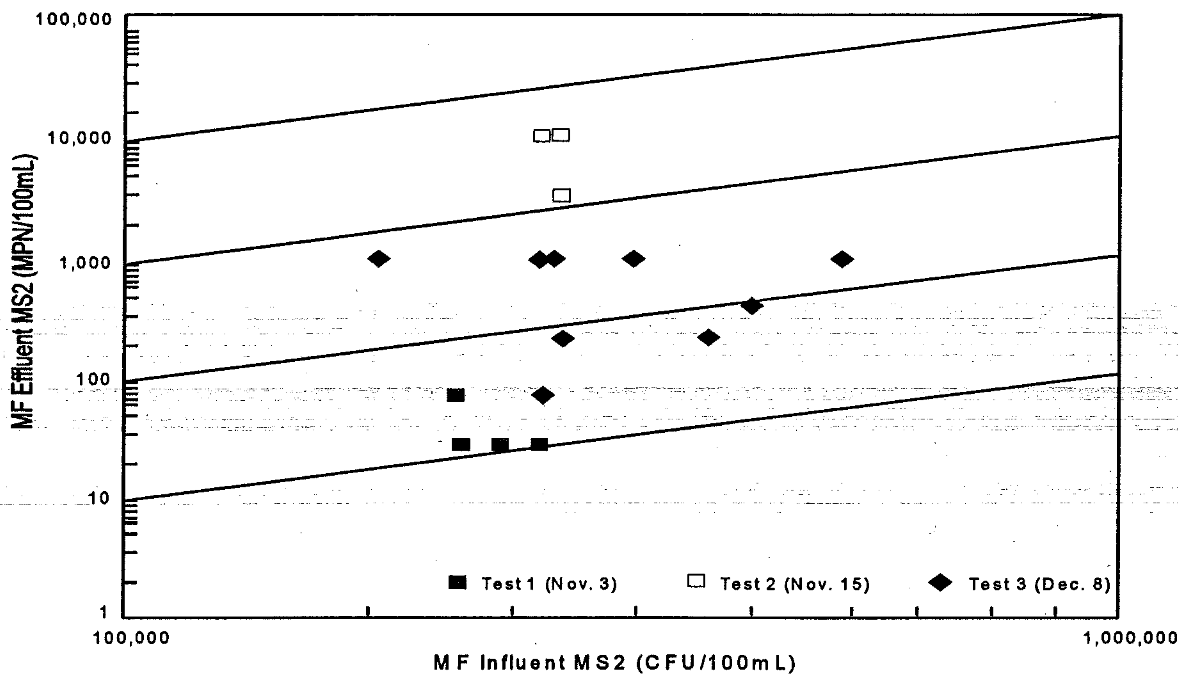

Figure 2—Removal of MS2 phages for microfiltration, Southeast Plant, San Francisco.

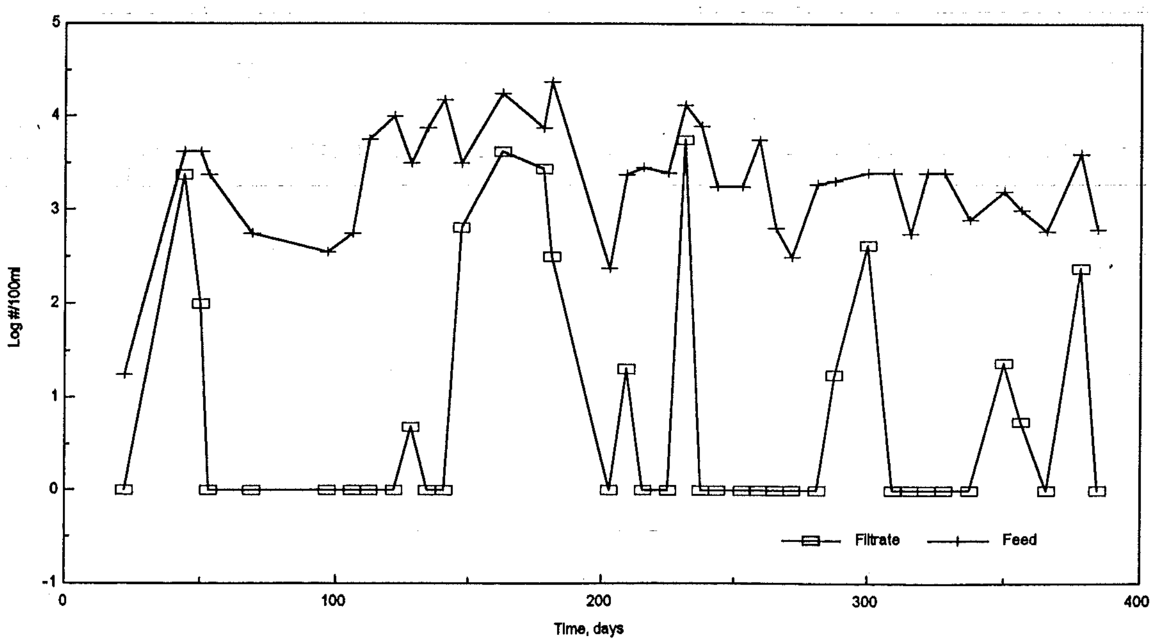

Figure 3—Removal of MS2 phages for Memcor microfiltration, Back River WWT Plant, Baltimore.

ANOMALOUS UV IRRADIATION RESULTS

Table 2 is adapted from Jolis and Hirano, and shows the apparent dependence of virus inactivation on the number of lamp banks through which the water passes, but not on the estimated dose within each bank. These data were recorded using a pilot scale UV disinfection unit with three banks of lamps arranged in a serpentine configuration. Samples were obtained after each bank and assayed for viruses, as described above.

Table 2---MS2 phage inactivation, Southeast Plant, San Francisco.

Date	Pass	Dose (mW-sec/cm²)	Removal (log)
Nov. 15	1	27	1.57-2.07
		37	1.57
	2	54	1.57-2.32
		75	1.57-2.59
		91	1.57-2.32
	3	81	2.32-2.59
		112	2.59-3.00
		137	2.59
Nov. 19	1	29	2.25
		35	2.25
		40	2.25
		46	2.25
		50	2.25
	2	58	2.25
		70	2.45
		81	2.66
		91	2.99
		100	2.99
Nov. 20	1	32	<1.80
		38	2.50
		43	2.50
		48	2.50
		53	2.50
	2	63	2.40
		75	2.50
		86	2.20
		96	2.90
		107	3.30
Nov. 21	1	37	1.69
		44	1.64
		53	0.00
		61	1.81
		76	1.60
	2	74	--
		88	3.21
		106	2.00
		122	3.39
		152	3.17

It is clear that excellent UV inactivation is observed with doses well below the 140 mW-s/cm² recommended to meet the disinfection standard in Title 22 of the California Code of Regulations, as noted in the Introduction. However, the apparent dose-independence within one bank is incompatible with the generally accepted disinfection mechanism in which a single UV photon in the effective wavelength is enough to dimerize adjacent thymine bases in the viruses's genome. As such events are independent of each other, it is easy to show that they imply that an initial virus population N_0 will be reduced by a dose D to $N(D)=N_0\, e^{-kD}$ where k is a constant (Darby, 1993; Loge, 1996)

The combination of experimental and theoretical support for the validity of this mechanism on the microscopic level is so strong that the most plausible interpretation of the apparent dose independence, which might reasonably be called the "Jolis-Hirano effect" is that it is an illusion resulting from macroscopic hydrodynamics that invalidates simple methods of estimating the average dose to the water.

If lamp intensity is a constant, I, then for an exposure time t, the dose is $D = It$. However, if I is a function of time, $I(t)$, then for exposure from t_1 to t_2,

(1)
$$D = \int_{t_1}^{t_2} I(t)\, dt \quad .$$

Moreover, if plug flow does not hold within a lamp bank, then not every volume element of water spends the same time within the bank. On the assumption of plug flow, the manufacturer of the disinfection unit, Trojan Technologies, provided the following formula relating D to flow, Q and $\%T$, the percentage transmittance of the water at the wavelength of the UV lamps (253.7 nm):

(2)
$$D = (1344/Q)\, e^{(.0263 \times \%T)} \quad .$$

Since $\%T$ was nearly fixed at around 67% in Jolis and Hirano's measurements, estimated D was almost inversely proportional to *Q*. Moreover, from *Q* and the channel dimensions one can calculate the average velocity. Thus, although Jolis and Hirano put only their *D* estimates in these tables, it is possible to compute the approximate *Q* and velocity values that correspond.

One observes that their "high-dose" observations correspond to relatively low average flow velocities upstream and downstream of lamp banks, as shown in Table 3. These average flow velocities are upper bounds for the velocity near wetted surfaces where viscous effects have increased importance, and thus they are lower bounds for the mean velocities in the regions that are well away from solid surfaces.

Table 3—Average flow velocities for estimated doses, using eq. (1), and dimension of UV pilot unit, Southeast Plant, San Francisco.

Single bank dose (mW-sec/cm^2)	Flow		Velocity outside lamp banks (cm/sec)
	(gpm)	(l/sec)	
27.0	95.5	6.0	26.7
32.0	80.6	5.1	22.7
37.0	69.7	4.4	19.6
44.0	58.6	3.7	16.4
48.0	53.7	3.4	15.1
53.0	48.6	3.1	13.8
61.0	42.3	2.7	12.0
76.0	33.9	2.1	9.3
95.5	27.0	1.7	7.6

The difference implies that most of the water does not flow close to the surfaces, which has three consequences. First, the reduced effective cross-sectional area in the banks increases the velocity of flow of most of the water; Second, the higher velocity reduces the water's exposure time compared to what one expects from assuming that plug flow extends to the surfaces of the lamps; Third, the average distance from the lamps to the region of most rapid flow is also larger than one would expect from uniform plug flow, so that the intensity is decreased by the absorbance in the water. Thus, departures from plug flow reduce the dose and hence the effectiveness of disinfection for most of the water. Enhancement of these effects with decreasing flow velocities would account for the apparent dose-independence of disinfection in this type of experiment.

THE HUGE CHANNEL STUDY

Support for this reasoning is provided by examination of the experimental results reported by Blatchley, et al. (1995). They used for their horizontal lamp test a 64-lamp array in a channel 60 cm wide filled to a depth of 60 cm (2 feet), as shown in Figure 4.

This array of eight modules, of eight lamps each, made the interlamp spacings and the spacings between the lamps and the channel sides and bottoms the same as in the smaller channels, so that hydraulic conditions within the large array were similar to those in the smaller arrays.

Two sets of measurements were taken along vertical lines at the centerline of the channel. Thus, effects of the sides could not be observed, but boundary layer effects appear in some measurements made only a few centimeters from the bottom. In one set of data, measured with the horizontal lamp array, the depth, as noted above, was about 60 cm, so that the channel cross-section downstream of the lamps was ~ 60 x 60 cm, for an area of ~3600 cm^2, and at a flow of 70.1 L/sec, the average velocity in this region was therefore ~19.5 cm/sec.

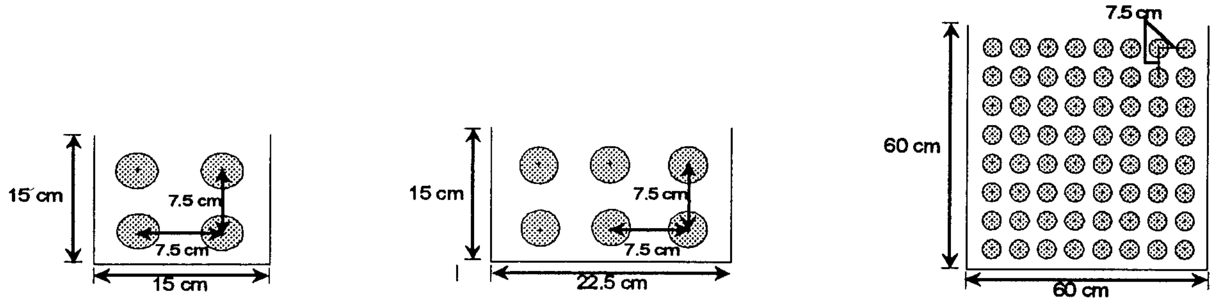

a) Loge, et al., and Jolis/Hirano (b) Anderson and Tchobanoglous (c) Blatchley, et al.

Figure 4---Cross sections of lamp arrays used in different experiments.

These data show barely a hint of slowing in the measurement closest to the bottom, at a height of ~ 4 cm, as shown in Figure 5(a). The other measurements were made with vertical arrays of lamps, so that the channel was filled to a depth of 150 cm, giving a cross-section outside the lamp arrays of ~ 9000 cm^2. The flow rate in this case was 87.6 L/sec for an average velocity of ~ 9.7 cm/sec; at this velocity the bottom boundary layer is clearly more than 5 cm thick, as seen in Figures 5(b) and 5(c). These two average flow velocities evidently are close to the velocities estimated in Table 3 for Jolis and Hirano's estimated single-bank doses of, respectively, 37 and 76 mW-s/cm^2. Thus, at single-bank doses between these two values, which include the majority of Jolis and Hirano's measurements, one must infer boundary layers several cm thick not only along the channel bottom, but also along the sides and the lamp sleeves. This is a significant fraction of the lamp spacing, since the lamps are arranged with their centers about 7.5 cm apart, but the 2.5 cm outside diameter of the quartz sleeves of the lamps makes the minimum distance between sleeve surfaces ~5 cm.

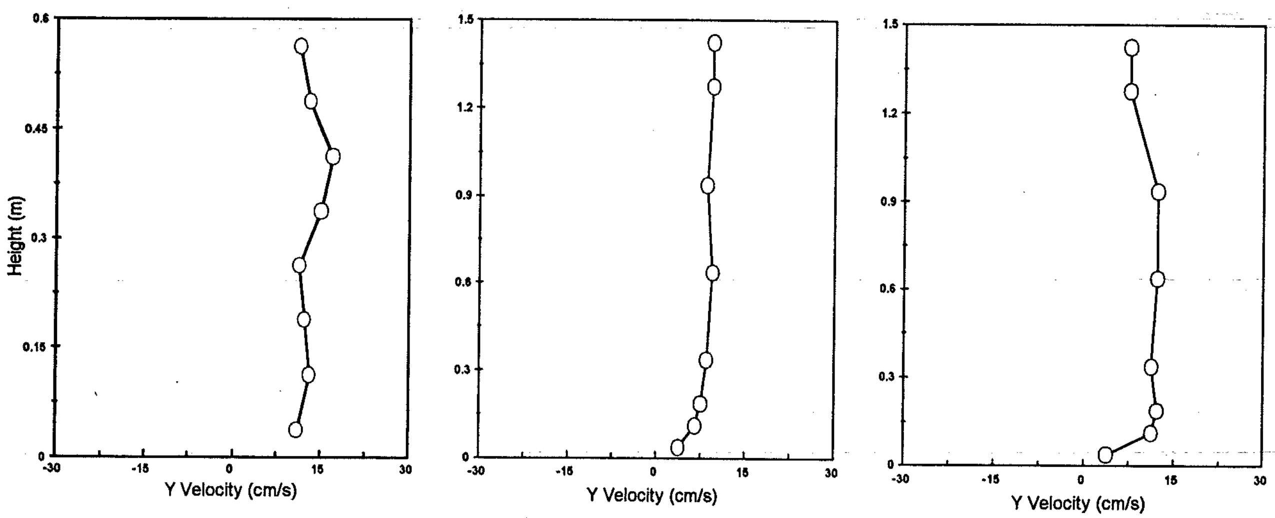

(a) horizontal, downstream (b) vertical, between arrays (d) vertical, downstream

Figure 5---Velocity profile for vertical and horizontal lamp configuration.

The average flow velocities in Table 3 and in this section are calculated outside the lamp banks to allow comparisons that are free of the disturbing effects of the lamps. Since the cross-sectional area of one lamp with its sleeve is ~ 4.9 cm^2, if plug flow extended to all surfaces then the water would flow at velocities near the average velocity, which would be increased by about 8% from the values above and in Table 3, corresponding to the area reduction imposed by the lamp and sleeve assemblies. The added complexity of the additional boundary layers implies that most of the water is not flowing at this average velocity in the lamp banks.

THE ORANGE COUNTY HYDRAULIC STUDY

Anderson and Tchobanoglous (1995) is not only a discussion of the authors' experimental procedure and results, but also provides their readers with an extensive summary of the general methodology of hydraulic testing. Thus, although their brief analyses conclude that despite some departures from uniformity, the Trojan UV2000 pilot scale disinfection system operated with a satisfactory approximation to plug flow, they provide the information necessary to show that their results are consistent with the hypothesis of substantial boundary layer effects at low flow velocities.

Two sets of measurements were done: one with the dye injected immediately before the first bank, and one with the dye injected ahead of a baffle plate in the inlet box of the UV channel, several feet ahead of the first bank. All measures of the hydraulic characteristics of the UV 2000 are derived from the curves of dye concentration as a function of time (the F-curves) or their derivatives, the residence time distribution (RTD) curves.

The key parameters are:

a) The Morrill Dispersion Index (MDI), derived from the F-curve, MDI ≥ 1 by definition, and MDI ≤ 2 is considered by Anderson and Tchobanoglous to be acceptably close to plug flow;
b) T, the theoretical residence time, computed from the flow rate and channel volume;
c) θ, the mean residence time, computed from the RTD curve;
d) t_p, the time of the peak of the RTD curve, counted from the beginning of the dye injection;
e) t_{50}, the median of the RTD curve, also from the beginning of injection.

They are tabulated in Tables 4 and 5.

Table 4—Parameters from RTD curve for the Trojan UV 2000 pilot-scale system for injection at the first UV light bank, Orange County.

Parameter	Effective plug flow	60 gal/min			120 gal/min			180 gal/min		
		Bank 1	Bank 2	Bank 3	Bank 1	Bank 2	Bank 3	Bank 1	Bank 2	Bank 3
θ, s	--	29.51	44.08	62.81	24.26	32.73	42.47	24.11	29.16	36.17
T, s	--	29.05	48.13	67.87	22.58	32.73	43.05	20.59	28.01	35.36
t_{90} / t_{10}	<2.0	1.27	1.17	1.15	1.24	1.20	1.20	1.34	1.22	1.21
d	0.01→0.10[(a)]	0.12	0.08	0.10	0.14	0.10	0.10	0.19	0.10	0.10
t_i / T	1.0	0.81	0.77	0.80	0.89	0.82	0.82	0.95	0.89	0.85
t_p / T	1.0	1.00	0.91	0.91	1.04	0.96	0.95	1.12	1.04	1.00
θ / T	1.0	1.02	0.92	0.93	1.07	1.00	0.99	1.17	1.04	1.02
t_{50} / θ	1.0	0.99	0.99	0.99	0.98	0.98	0.99	0.96	0.99	0.99
σ^2	--	7.43	7.75	12.55	7.14	6.53	8.93	9.26	6.34	7.55
σ_θ^2	--	0.25	0.17	0.20	0.29	0.20	0.21	0.38	0.21	0.20
E	--	334.45	503.35	859.68	703.32	1077.80	1731.34	1236.42	1627.67	2439.79
L / D	15.0	23.04	23.04	23.04	23.04	23.04	23.04	23.04	23.04	23.04

(a) Moderate dispersion

Table 5—Parameters from RTD curve for the Trojan UV 2000 pilot-scale system for injection at inlet box, Orange County.

Parameter	Effective plug flow	60 gal/min			120 gal/min			180 gal/min		
		Bank 1	Bank 2	Bank 3	Bank 1	Bank 2	Bank 3	Bank 1	Bank 2	Bank 3
θ, s	--	46.28	60.31	77.85	32.63	42.42	50.40	33.69	39.48	46.17
T, s	--	48.15	67.23	86.97	33.09	43.24	53.56	28.45	35.87	43.22
t_{90} / t_{10}	<2.0	1.54	1.24	1.16	1.34	1.22	1.17	1.54	1.32	1.37
d	0.01→0.10[(a)]	0.80	0.33	0.20	0.34	0.19	0.13	0.43	0.27	0.36
t_i / T	1.0	0.73	0.76	0.77	0.79	0.81	0.80	0.88	0.84	0.86
t_p / T	1.0	0.89	0.89	0.91	0.95	0.97	0.92	1.12	1.07	1.03
θ / T	1.0	0.96	0.90	0.90	0.99	0.98	0.94	1.18	1.10	1.07
t_{50} / θ	1.0	0.95	0.97	0.99	0.96	0.99	0.99	0.95	0.97	0.97
σ^2	--	74.67	40.51	31.87	22.43	16.84	13.47	29.50	21.42	33.69
σ_θ^2	--	1.61	0.67	0.40	0.68	0.39	0.26	0.87	0.54	0.73
E	--	4207.40	2746.82	2247.94	3227.23	3063.85	2809.53	5516.44	5795.41	10873.79
L / D	15.0	23.04	23.04	23.04	23.04	23.04	23.04	23.04	23.04	23.04

(a) Moderate dispersion

Anderson and Tchobanoglous explain that these parameters were originally developed for studying settling basins, where three particular ratios have simple physical meanings. $\theta/T < 1$ implies dead space, which is a region that does not participate in the flow through the basin. Likewise, $t_p/\theta < 1$ and $t_{50}/\theta < 1$ indicate short-circuiting, in which water flowing along some paths in the active volume spends less time in the basin than water flowing along other paths. It is also worth noting that $\theta/T > 1$ is impossible if T is calculated from the correct volume, but that underestimating the volume may easily occur in an open-topped channel in which headloss produces a depth gradient.

The authors assert that there is little or no dead space or short-circuiting in a UV reactor, and they therefore interpret their results more generally as indicating nonuniform flow. However, the difference in flow rates expected between boundary layers and the regions farther from wetted surfaces resembles the difference between long or short paths in a settling tank, and the slowest moving portions of boundary layers are nearly dead space. Thus, the boundary layer hypothesis predicts that $t_p/\theta<1$ and $t_{50}/\theta<1$ for all measurements of the UV channel. Out of a total of eighteen sets of measurements (two dye injection modes, three banks, and three flow rates) $t_p/\theta<1$ in sixteen of the eighteen, $t_p/\theta = 1$ in one, and $t_p/\theta = .91/.90$ in the last case, which probably is not significantly greater than 1. t_{50}/θ is less than one in all measurements.

The comparison with T is more difficult because of the possibility that T may not have been correctly adjusted for the change in volume with changing flow rates. Anderson and Tchobanoglous note that the channel bottom sloped downward irregularly as in Table 6a and that after adjusting for the slope in the bottom there was a headloss in each bank, as shown in Table 6b, such that the actual volume in each lamp bank had an increasingly trapezoidal longitudinal profile with increasing flow. Underestimation of volume and hence *T* is the probable explanation why $\theta/T > 1$ for all banks and both injection modes at 180 gpm. The greater depth in bank 1 may also contribute to the values of θ/T being larger in this bank than in the other two banks at the lower flow rates. Thus, although θ/T increases with increasing flow rate in a way that is consistent with the hypothesis, the specific numbers appear too dubious to justify further discussion.

Table 6a---Depth measurements in Trojan UV 2000 pilot-scale system at zero flow rate, Orange County.

Depth bank 1 (in)		Depth bank 2 (in)		Depth bank 3 (in)	
Before	After	Before	After	Before	After
4.38	4.50	4.53	4.75	4.81	5.00

Table 6b---Adjusted depth measurements for establishing head losses in Trojan UV 2000 pilot-scale system, Orange County.

Flowrate (Gpm)	Depth bank 1 (in)		Depth bank 2 (in)		Depth bank 3 (in)	
	Before	After	Before	After	Before	After
60	5.81	5.75	5.75	5.69	5.69	5.63
120	6.44	6.25	6.25	6.06	6.06	5.88
180	7.31	6.88	6.88	6.44	6.44	6.00

COMPUTATIONAL STUDIES

Laboratory fluid dynamic studies of UV lamp arrays in more detail than studies like those in Anderson and Tchobanoglous are possible, but they are likely to be very expensive. It is likely to be more cost-effective to seek further insight into fluid flow in the lamp arrays by a computational simulation, because software that can support such studies on workstations or high-end personal computers is now widely available and relatively inexpensive.

The conventional approach to such simulations is of course the finite-element method, in which a solid volume is subdivided into many tetrahedra or parallel-pipeds, on each of which is evaluated a linear approximation to a solution of the Navier-Stokes equation.

For the calculations needed to explore the hypothesis about the effect of boundary layers, the calculation would be relatively simple, since the channel would be rectangular and one could begin by merely including cylindrical voids in the water volume to represent the lamps. The elements would be smaller near the wetted surfaces to provide higher resolution of the flow there, and the sizes and shapes of the elements might be adjusted to the input flow velocity because of the changing thicknesses of the boundary layers.

Simulation at this basic level of approximation could test the validity of a simplified concept, depicted in Figure 6. The spacing among the lamps and between the lamps and the channel boundaries allows any cross-section through any bank in any of the channels in Figure 4 to be subdivided so that each lamp is surrounded by a square that is 7.5 cm on a side. Then the area not occupied by the lamp is

(3) $$(7.5\ cm)^2 - \pi(1.25)^2\ cm^2 \approx 51.34\ cm^2.$$

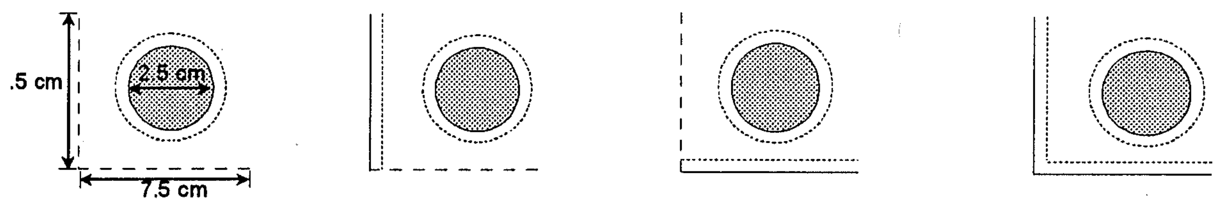

(a) Lamp only (b) Lamp and side (c) Lamp and bottom (d) Lamp and corner

Figure 6—Cross sectional views of simplified boundary layer configurations.

Table 7 shows the available area if a static layer of s specified thickness exists around the lamp alone, or around the lamp and one or two sides of the square, to represent the effect of a side and/or the bottom of the channel. This binary division of the area into static and freely flowing regions is only a schematic approximation of the actual situation in which continuous gradations occur, but it provides easily calculated values for possible degrees of deviation from the assumption of plug flow extending to all wetted surfaces, and may be useful to compare with the results of computational simulations and laboratory tests.

Table 7—Effective area after reduction by boundary layer, based on figure 6.

Boundary layer thickness (mm)	Effective area (cm^2)		
	Lamp only	Lamp and one side	Lamp and corner
0.00	51.34	51.34	51.34
2.50	49.18	47.30	45.49
5.00	46.63	42.88	39.38
7.50	43.68	38.06	32.99
10.00	40.35	32.85	26.35
12.50	33.62	24.24	16.43

ANGLED VANES TO ENHANCE PLUG FLOW

Although the studies described in the previous section are desirable to verify the boundary layer hypothesis, the evidence for it appears sufficiently strong now that it seems worth considering a possible modification of conventional UV reactor design to counteract the formation of boundary layers. The aircraft industry has long used arrays of small vanes strategically located on wings to control the formation of boundary layers. By setting the vanes at small angles to the flow, as shown in Figure 7a, angled alternately left and right, areas of widening and narrowing cross-section are formed that respectively decelerate and accelerate the flow, thus interfering with the uniformity of motion needed for boundary-layer formation.

Evidently, the same approach might plausibly be applied in a UV reactor, so that something like Figure 7b would result, with vanes attached to the sides and bottom of the channel. Small collars with vanes can also be fabricated easily to snap onto or slip over the quartz lamp sleeves as indicated in Figures 7c and 7d.

However, since the fluid dynamic regime for water flowing ~ 10 cm/sec is very different from that of air flowing over aircraft wings, one could not expect the parameters of aircraft vane arrays (such as vane length, height, angle to the flow, and the spacing between them) to be appropriate for a UV reactor. Thus, testing different configurations and optimizing the parameters is another task that should be done by computation.

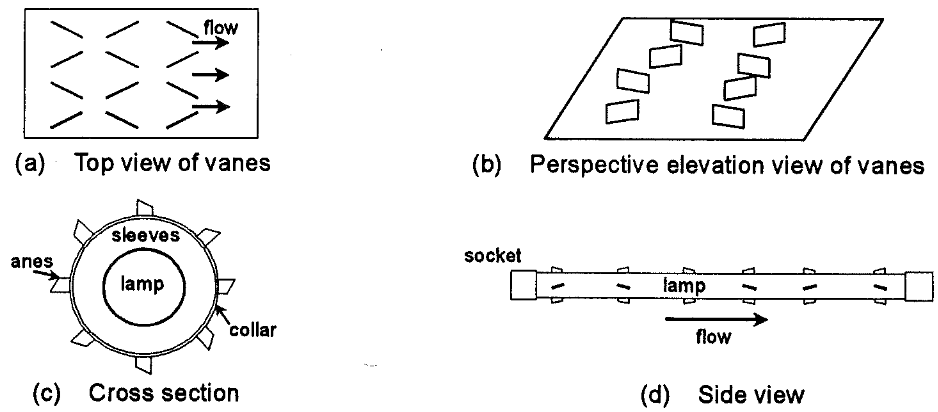

Figure 7—Example of vane array for plug flow enhancement, NTS.

Once computation had arrived at a satisfactory design, the next step would be to proceed with hydraulic and disinfection tests.

CONCLUSION

The boundary-layer hypothesis implies that in Jolis and Hirano's experiment most of the water that supposedly received a dose of 88 mW-s/cm^2 actually received much less. Hence, if some modification of UV disinfection design, such as the one proposed here, maintained a closer approximation to plug flow at lower velocities, it might be possible to meet the Title 22 virus standard for disinfected reclaimed water with a dose of 70 mW-s/cm^2 or less, and a consequent large saving in both energy and capital costs from a unit designed for 140 mW-s/cm^2. If the performance of a microfiltration unit in removing viruses could be stabilized at the levels that are sometimes reached, as described in the experimental results in the first part of this paper, then the burden on the UV unit could be reduced further. It appears that combined MF/UV systems have the potential for much better efficiency, and that at least the improvement of UV disinfection will not be excessively difficult to achieve. It is obvious that such improvements would be both technically and economically desirable.

ACKNOWLEDGMENTS

Authors are manager and technical staff of Wastewater Engineering Services and the manger of Terminal Island Treatment Plant of Los Angeles Sanitation. For correspondence, contact R. Iranpour, Principal Investigator, of Research Group at: P.O. Box 806; Culver City, CA 90232.

REFERENCES

Adams, M.H. (1958) *Bacteriophages*. Intersciences Publishers. New York.

Anderson, J., and Tchobanoglous, G. (1995) Hydraulic Characterization of the Trojan UV 2000 Pilot-scale Disinfection System, Green Acres Water Reclamation Facility, Orange County Water District, Fountain Valley, California.

Blatchley III, E.R., Wood, W.L., and Schuerch, P. (1993) "Large-scale Pilot Investigation of Ultraviolet Disinfection." *Proc., WEF Specialty Conf. Series on Plng., Des., and Operations of Effluent Disinfection Systems*. pp. 417-432.

Blatchley III, E.R., Wood, W.L., and Schuerch, P. (1995) "UV Pilot Testing: Intensity Distributions and Hydrodynamics." *ASCE J. of Envir. Eng.* Vol. 121, No. 3.

California Administrative Code, Title 22, Division 4 (1978) Wastewater Reclamation Criteria. Department of Health Services, State of California, Berkley, CA.

Darby, J.L., Snider, K., and Tchobanoglous, G. (1993) "Ultraviolet Disinfection for Wastewater Reclamation and Reuse Subject to Restrictive Standards." *Water Envir. Research.* Vol. 65, No. 2, pp. 169-180.

Emerick, R.W., and Darby, J.L., (1993) "Ultraviolet Disinfection of Secondary Effluents: Predicting Performance Based on Water Quality Parameters." *Proc., WEF Specialty Conf. Series on Plng., Des., and Operations of Effluent Disinfection Systems.*

Iranpour, R., et al. (1998) "Virus Removal by Advance Membrane Filtration for Wastewater Reclamation." *Water Envir. Research*, in press.

Iranpour, R., et al. (1997) "of: UV Pilot Testing: Intensity Distribution and Hydrodynamics." *ASCE J. Envir. Eng.*, Vol. 123, No. 5, pp. 521-523.

Iranpour, R., et al. (1998) "of: Wastewater Reclamation at Lake Arrowhead, California: An overview." *Water Envir. Research*, in press.

Jolis, D. and Hirano, R. (1993) Microfiltration and Ultraviolet Light Disinfection for Water Reclamation. Bureau of Engineering, Department of Public Works. City and County of San Francisco.

Loge, F.J. Emerick, R.W., Heath, M., Jacangelo, J., Tchobanoglous, G., and Darby, J.L. (1996) "Ultraviolet Disinfection of Secondary Wastewater Effluents: Prediction of Performance and Design." *Water Envir. Research.* Vol. 68, No. 5, pp. 900-916.

Schwartzel, D.T. and Sakamoto, G. (1996) "Pilot Testing High-Intensity UV Lamp Technology to Meet California Wastewater Reclamation Criteria. " *Proc., WEF Specialty Conf., Disinfecting Wastewater for Discharge and Reuse.* Portland, Oregon.

Water Board, Sydney, Illawarra and Blue Mountains, New South Wales, Australia; and Memtec Limited, Windsor, New South Wales, Australia (1992). Demonstration of Memtec Microfiltration for Disinfection of Secondary Treated Sewage. Water Board; Department of Industry, Technology and Commerce; and Memtec. New South Wales, Australia.

Willinghan, G.A., Olivieri, V.P., Vickers, J.C., McGahey, C.L. (1992) Field Evaulation of Continous Microfiltration for Tertiary Wastewater Treatment, preprint, Memtec America Corporation, Timonium, MD.